ISSN: 0067-2904

Synthesis and Structural Views on New Azo Ligand and Its Metal Complexes with Some of their Application

Asmaa Edrees Fadhil*, Alyaa Khider Abbas
Department of Chemistry, College of Science, University of Baghdad, Baghdad, Iraq

Received: 17/10/2022 Accepted: 6/2/2023 Published: 30/12/2023

Abstract

In this work, we presented a study of the structural formula for a new series of complexes with Ag(I), Cu(II), Zn(II), and Cd(II) derived from the guanine azo dye ligand 2-amino-8-((3-hydroxyphenyl)diazinyl)-1,7-dihydro-6H-purin-6-one (HAG), which is investigated using various physicochemical analyses, spectroscopic techniques (FT-IR, U.V-VIS, and ^{1}H NMR), thermogravimetric analysis (TGA). In addition, elemental analyses, magnetic susceptibility, and molar conductance measurements were all stabilized. As well as the mole ratio, stability constant, and Gibbs free energy were studied for all complexes, where they showed high stability and spontaneous synthesis. The Cu(II) complex was suggested to have octahedral stereochemistry, while the Ag(I), Zn(II), and Cd(II) complexes were suggested to have tetrahedral stereochemistry. The ligand has been demonstrated to be a useful acid-base indicator, and it has been shown that the ligand (HAG) and its complexes exhibit high photostability and have various colors that can be used to dye wool materials.

Keywords: Guanine azo, Photostability, Physicochemical, Dye wool, Acid-base indicator

تحضير واراء في الهيكلية لليكند ازو جديد ومعقداته مع بعض التطبيقات.

أسماء ادريس فاضل* ، علياء خضر عباس
قسم الكيمياء، كلية العلوم، جامعة بغداد، بغداد ، العراق

الخلاصة

في هذا العمل، قدمنا دراسة الصيغة الهيكلية لسلسلة جديدة من المعقدات Cd(II) Zn(II), Cu(II), Ag(I) مشتقه من ليكند كوانين ازو 2-amino-8-((3-hydroxyphenyl)diazinyl)-1,7-dihydro- (HAG) 6H-purin-6-one], و تم فحصه باستخدام التحليلات الفيز و كيميائية و تقنيات التحليل الطيفي (FT-IR، UV-VIS و ^{1}H NMR) ، التحليل الحراري الوزني (TGA) . بالإضافة إلى ذلك، تم قياس جميع التحليلات الأولية للعناصر، و القابلية المغناطيسية، و قياسات الموصلية المولية. و كذلك دراسة النسبة المولية و ثابت الاستقرار و طاقة جيبس الحرة لجميع المعقدات حيث أظهرت استقراريه عالية و تحضيرها تلقائي. معقد Cu(II)له الشكل الفراغي ثماني السطوح بينما معقدات Ag(I),Zn(II),Cd(II) لهم الشكل الفراغي رباعي السطوح. لقد وجد ان الليكاند له القابلية ان يسلك سلوك دليل حامض- قاعدة كما انه و معقداته لهم استقراريه ضوئية عالية و قابلية جيدة للعمل كأصباغ لصباغة الانسجة القطنية و ذلك لألوانهم المتعددة.

*Email: asmaa.idrees1205m@sc.uobaghdad.edu.iq

1. Introduction

Guanine is an organic compound that belongs to the purine group, which is made up of a fused pyrimidine-imidazole ring system comprising carbon and nitrogen atoms. Azo dyes make up most dye chemistry production today, and in the future, their relative importance might increase. They are necessary for developing the printing and dye markets. These dyes are produced using a simple coupling of the diazotization process. A number of changes and detours are taken in order to achieve the desired results. Greater dispensability, yield, and dye particle size are important dye characteristics. Azo dyes provide more than 60% of the colors used in contemporary dyes [1]. The majority of industrial colors-roughly 70% are synthetic azo dyes. These substances are distinguished by the functional group (-N=N-) connecting symmetrical or asymmetrical fragments. Azo dyes are utilized as a more important material for the textile and printing industries that disperse colors. Additionally, they have been used in various fields, including electro-optical devices, liquid crystal displays, nonlinear optics, cosmetics, food coloring, acid-base indicators, and polymers [2]. The study aims to synthesize and characterize a new ligand (HAG) and its complexes with Ag(I), Cu(II), Zn(II), and Cd(II), as well as to investigate its ability to dye cotton fabric. Acid-base indicators and photostability were investigated.

2. Experimental

2.1. Materials and instruments

All chemicals were purchased from commercial sources and used without additional purification unless stated otherwise. Elemental microanalysis of the HAG ligand were recorded on a Eure EA 3000 Elemental Analyzer. The pH values of the samples were measured using HANNA instruments. The FT-IR spectral data were recorded using a Shimadzu 8400s spectrophotometer. The UV-Vis spectral data were recorded using a Shimadzu 1800 UV-Vis spectrophotometer. ^{1}H NMR spectral data were recorded using a Bruker AV400 Avance-III spectrometer. Thermal gravimetric analysis (TGA) was utilized to measure the metal content of the synthetic ligand and complexes by SDT, Q600 V20.9 Build. Melting points are uncorrected and were recorded in open capillary tubes using a Gallenkamp instrument. The molar conductance of metal ion complexes was examined at 10^{-3} M in deionized distilled water. The Mohr method was used to determine the chloride concentrations in the complexes. The magnetic susceptibilities of the complexes were assessed at room temperature using a Sherwood scientific auto-magnet susceptibility balance model.

2.2. Synthesis of 2-amino-8-((4-chloro-3-hydroxyphenyl)diazinyl)-1,7-dihydro-6H-purin-6-one)ligand

To a solution of 4-amino-2-chlorophenol (2.23 g, 0.01 mol) in EtOH (30 mL), concentrated acetic acid (4 mL) was added at 0-5 °C [2]. A cooled solution of sodium nitrite (0.83 g, xx mol) in water (25 mL) was slowly added to the reaction mixture with stirring at 0-5 °C. The solution of diazonium salt was then added to a cold solution of guanine (1.94 g, 0.01 mol), which was dissolved in an ethanolic NaOH solution (14 mL, 10%). The resultant mixture was neutralized to pH 5-6 by either adding acetic acid or sodium hydroxide. The colored precipitate was filtered, washed with water: ethanol (1:1) , then collected and dried. The preparation method of an azo ligand is shown in Scheme 1 [3]

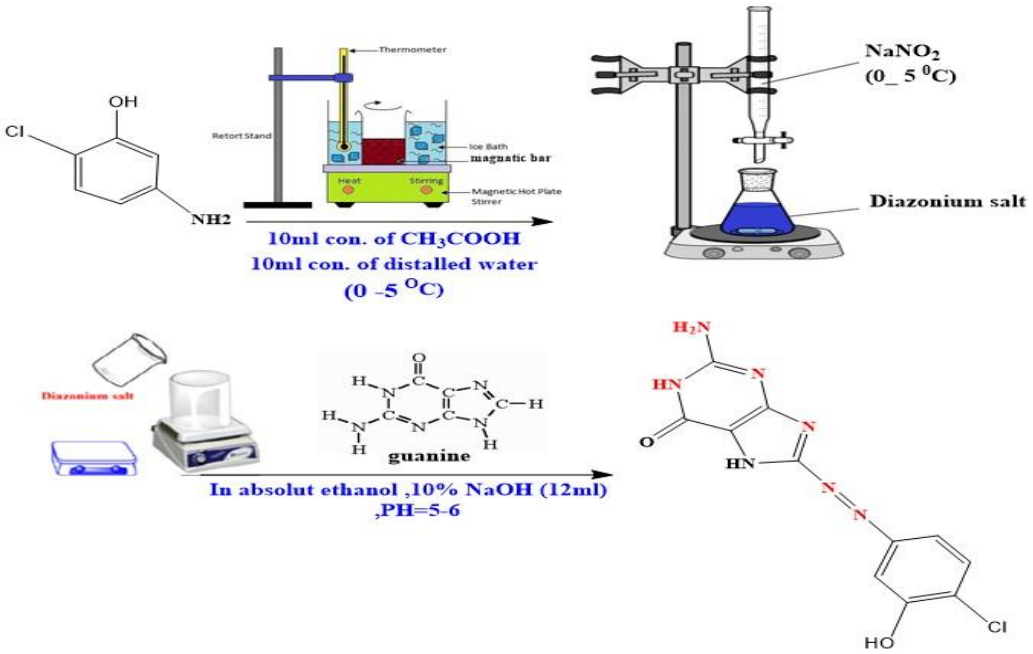

Scheme 1 : The synthesis of the HAG ligand

2.3. Metal complex synthesis

All new complexes were synthesized in a mole ratio of M:L (1:1), except (Cu-HAG), which had a mole ratio of 1:2. The HAG ligand (0.306 g, 1 mmol) was dissolved in a minimal amount of deionized distilled water (Scheme 2). The ligand solution was gradually added to the appropriate aqueous solution of metal salts [$AgNO_3$ (0.1698 g, 1 mmol), $ZnCl_2$ (0.1362 g, 1 mmol), $CdCl_2$ (0.183 g, 1 mmol), or $CuCl_2.6H_2O$ (0.8524 g, 0.5 mmol)] in deionized distilled water. The reaction mixture was then heated to reflux for 3 hours, and the reaction was monitored by TLC using a mixture of solvents (0.8 mL of methanol, 1.2 mL of ammonia, and 4 mL of butanol). The solid crude material was filtered after washing the mixture with a mixture of deionized distilled water and ethanol. The physicochemical properties of the HAG ligand and its complexes are listed in Table 1 [4].

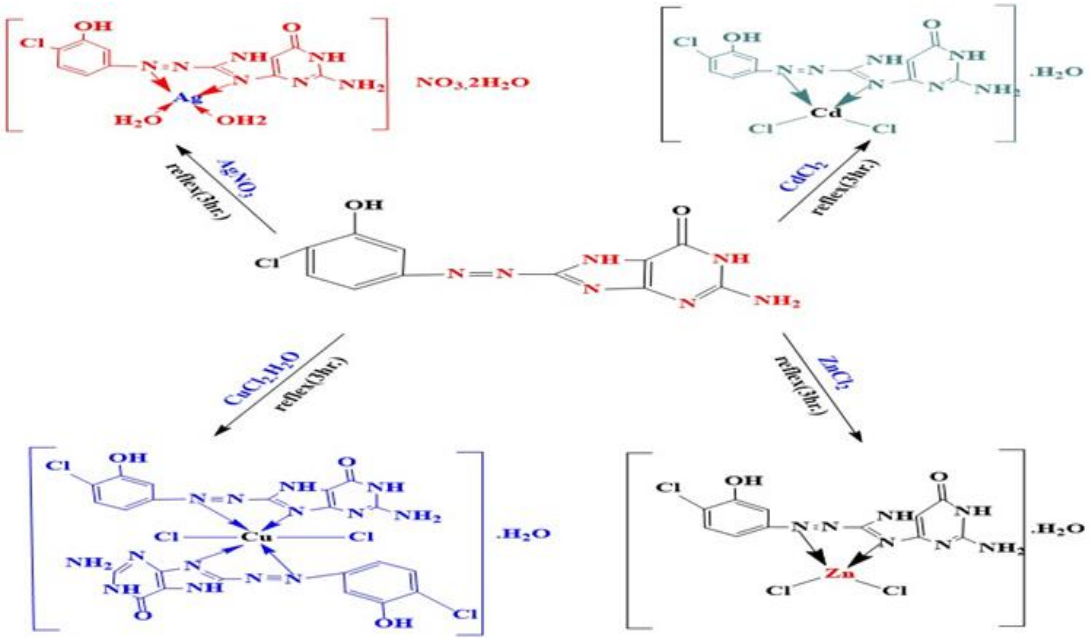

Scheme 2 : The synthesis of HAG complexes

Table 1: Some physical and chemical properties of the HAG ligand and its complex

No.	Compound (M.wt) (gm/mol)	Color and λmax (nm)	M:L	Λm ($S.mol^{-1}.cm^2$)	C.H.N Experimental (%) Theoretical (%)				
					C	**H**	**N**	**M**	**Cl**
1	$HAG(C_{11}N_7H_{10}O_2Cl)$ 306.76	Brown 339.00	-	-	48.661 48.012	4.608 4.712	36.994 36.127	-	8.569 8.325
2	$[Ag(HAG)(H_2O)_2]NO_3.2H_2O$ 548.58	Yellowish brown 447.00	1:1	55.7	25.325 25.726	3.593 3.508	19.648 19.100	21.020 21.521	12.382 12.547
3	$[Cu(HAG)_2Cl_2].H_2O$ 784.06	Green 597.00	1:2	24.6	37.330 37.023	3.240 3.365	27.195 27.487	8.910 8.852	9.950 9.025
4	$[Zn(HAG)\ Cl_2].H_2O$ 461.14	Yellowish orange 346.00	1:1	30.2	31.425 31.012	2.591 2.519	22.905 23.024	15.381 15.025	16.700 16.251
5	$[Cd(HAG)\ Cl_2].2H_2O$ 526.47	Yellowish brown 418.00	1:1	39.5	26.611 26.901	3.019 3.153	19.210 19.972	22.900 22.541	14.470 14.369

3. Result and discussion

All the synthesized compounds are stable across moisture, non-hygroscopic, and have bright colors. The structural formulae of the azo ligand and its metal complexes were confirmed by utilizing different physicochemical and spectroscopic techniques such as elemental analysis (C.H.N and M), molar conductivity, FT-IR, ^{1}H NMR, UV-Vis spectroscopy, magnetic magerment and thermal analysis. The elemental analysis and analytical results for metal complexes confirmed the formation of a M:L (1:2) mole ratio for the Cu(II) complex and were consistent with their suggested molecular formula, whereas the other complexes (M:L) have the mole ratio (1:1). By studying the molar conductivity of the complexes, it was found that all complexes are non-electrolytes, except for the silver complex, which has a 1:1 electrolyte (Table 1). The mole ratio approach, which was used, is the most common method for determining the composition of a complex in solution. The solutions were prepared at a concentration of 10^{-4} M. Figure 1 depicts the procedure and the locating outcomes, and Table 2 presents the data on the results.

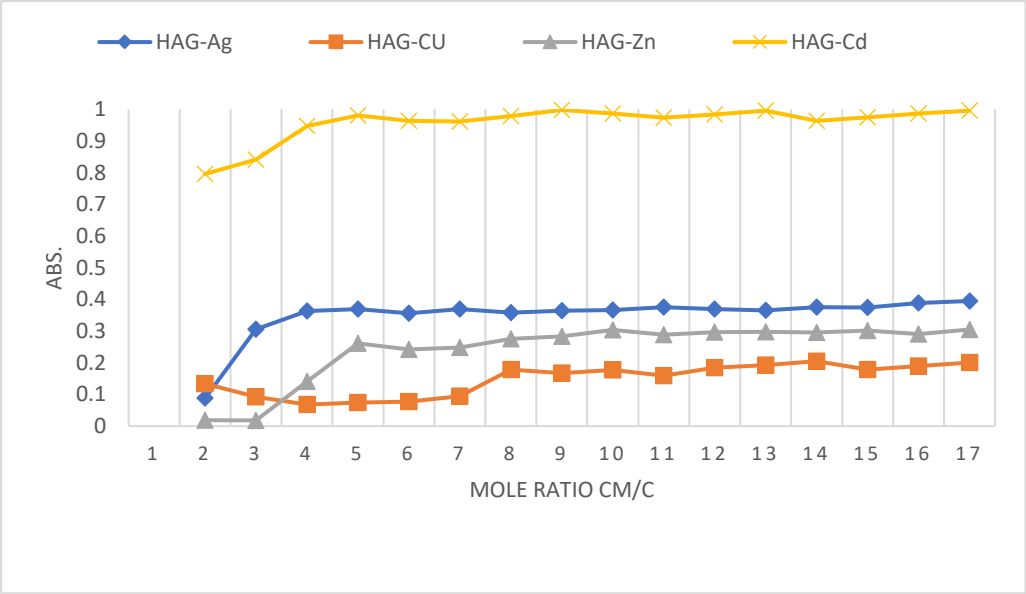

Figure 1: The mole ratio of HAG ligand and its complexes

Table 2: HAG-Metal ion solution absorbance *vs* mole ratio

M:L	Absorbance (λmax nm)			
	HAG-Ag 447	**HAG-Cu 600**	**HAG-Zn 334**	**HAG-Cd 418**
1:0.25	0.088	0.134	0.019	0.796
1:0.50	0.306	0.092	0.018	0.841
1:0.75	0.363	0.068	0.141	0.947
1:1	0.361	0.074	0.261	0.981
1:1.25	0.356	0.077	0.242	0.964
1:1.50	0.369	0.094	0.248	0.962
1:1.75	0.358	0.178	0.275	0.979
1:2	0.364	0.167	0.283	0.998
1:2.25	0.366	0.177	0.304	0.987
1:2.50	0.375	0.159	0.289	0.974
1:2.75	0.369	0.184	0.297	0.984
1:3	0.365	0.193	0.298	0.996
1:3.25	0.375	0.205	0.296	0.964
1:3.50	0.374	0.178	0.302	0.975
1:3.75	0.389	0.189	0.291	0.987
1:4	0.395	0.201	0.305	0.996

Spectrophotometric analysis can be used to estimate the stability constant [5]. The following formula was used to calculate the stability constant for Cu(II) complexes:

$$K = \frac{1-\alpha}{4\alpha^3 C^2} \qquad \text{where} \qquad \alpha = \frac{A_m - A_s}{A_m}$$

Where: α = The mole fraction of the reactant that submits dissociation is equal to the degree of dissociation.

As = the absorption of a solution with a stoichiometric (1:1) ratio (M: L).
Am = A solution's absorption, including excess ligand.
C = The mole/L concentration of the synthesized solution.
The stability constant for complexes Ag(I), Zn(II), and Cd(II) at a 1:1 ratio, on the other hand, was calculated using the following equation [6]:

$$K = \frac{(1-\alpha)}{\alpha^2 c}$$

According to the findings in Table 3, the stability is as follows, in ascending order:
$[Cu(HAG)_2Cl_2].H_2O$ > $[Cd(HAG)Cl_2].2H_2O$ > $[Ag(HAG)(H_2O)_2]NO_3.2H_2O$ > $[Zn(HAG)Cl_2].H_2O$
The thermodynamic coefficient of ΔG (Gibbs free energy) was obtained from the equation below [7]: $\Delta G = - RT \ln K$
Where: R is the gas's constant, and it is 8.31 J. $mole^{-1}$. K (T**)** is the temperature (Kelvin). The formations we obtained from G indicate that all complexes are synthesized spontaneously.

Table 3 : The behavior of the thermodynamic parameters of ΔG (Gibbs free energy)

Complex	As	Am	A	K	Ln K	ΔG(J/mole)
$[Ag(HAG)(H2O)_2]NO_3.2H_2O$	0.361	0.364	0.003	$110.7*10^5$	16.220	-40119.49
$[Cu(HAG)_2 Cl_2].H_2O$	0.074	0.167	0.556	$649*10^5$	17.988	-44492.40
$[Zn(HAG) Cl_2].H_2O$	0.261	0.283	0.022	$337.13*10^4$	15.030	-37177.20
$[Cd(HAG) Cl_2].2H_2O$	0.981	0.998	0.115	$386*10^5$	17.468	-43207.23

3.1. Thermogravimetric analysis (TGA)

The thermal behavior of the synthetic HAG ligand and its complexes is explored in Figure 2. Table 4 lists the estimated and discovered phase mass losses. In the four exothermic phases, the ligand HAG breakdown occurs in the 50-800 °C range. The first stage of decomposition occurs between 25 and 100 °C, resulting in a weight loss of 12.13%. The second stage occurs between 100 and 310 °C, resulting in a weight loss of 19.80%, and the third stage occurs between 310 and 400 °C, resulting in a weight loss of 8.958%. The final step of disintegration begins between 400 and 800 °C (25.39% weight loss) (as recommended in Figure 2A). In the case of $[Ag(HAG)(H_2O)_2]NO_3.2H_2O$ complex breaks down in the five stapes (Figure 2B). The initial stage of decomposition begins at 25 to 90 °C, resulting in a weight loss of 3.642% decomposed of water. At 90-249 °C, the second stages of breakdown were noticed (9.527% weight loss). Decomposition begins in its third stage at 249-390 °C (13.78% weight loss), moves to a range of 390-760 °C (25.22% weight loss) in the fourth stage. In the last stage (760-800 °C), the weight decreased by 44.13%. The chemical compound $[Cu(HAG)_2Cl_2].H_2O$, in contrast, breaks down into seven different components (Figure 2C). With a weight loss of 3.202%, the first stage of decomposition begins between 25 and 62 °C. The second stage of decomposition was recorded between 62 and 200 °C. Decomposition begins in its third stage between 200 and 400 °C (9.47% weight loss). In the fourth stage (400-500 °C), it was lost 10.79% of the weight. The fifth stage (weight loss of 19.30% at 500-625 °C). The sixth stage loses weight by 13.13% between 625-700 °C and 19.19% between 700-800 °C during the final stage of disintegration [6]. The Zn(HAG)Cl2.H2O complex is divided into five stapes (Figure 2D). At 25 to 60 °C, the first stage of decomposition begins, and a loss of 1.626 pounds results. The second stage of breakdown (14.17% weight loss) was noticed between 60 and 400 °C. Decomposition begins in its third stage between 400 and 475 °C (6.80% weight loss). Starting at the range 475-600 °C, the fourth stage lost weight by 10.51%, and the last stage reached 600-800 °C (weight loss of 22.0%). Considering $Cd(HAG)\ Cl_2.\ 2H_2O$ in five states, the complex breaks down (Figure 2E). At 25 to 85 °C, the first stage of breakdown begins, resulting in a

weight loss of 2.74%. The second stage of disintegration (5.24% weight loss) was seen between 85-220 °C. During weight loss of 220-400 °C (10.44%), the third stage of breakdown begins. At the range from 400 to 560 °C, the fourth stage started, losing weight by 11.93%. The final stage at 560-800 °C (weight loss of 27.69% [7]. The HAG ligand and its complexes (thermal stability) are reduced in the following order: $[Zn(HAG)Cl_2].H_2O$ (44.84%) > $[Ag(HAG)(H_2O)_2]NO_3.2H_2O$ (44.13%) > $[Cd(HAG)Cl_2].2H_2O$ (41.4%) > HAG (33.74%) > $[Cu(HAG)_2 Cl_2].H_2O$ (14.59%).

Table 4 : TGA of HAG ligand and their complexes

Compound	Molecular formula and molecular weight (g/mole)	Step	TG range of the decomposition (°C)	Suggested assignment	Mass loss (%)	
					Calculated (%)	**Found (%)**
HAG	$C_{11}H_{10}N_7O_2Cl$ 306.76	1	25-100	H_5Cl	12.16	13.10
		2	100-310	C_5H_5	19.80	20.79
		3	310-400	C_2	7.82	8.958
		4	400-800	C_4N_2	24.77	25.39
		Residue	>800	N_5O_2	33.25	33.74
$[Ag(HAG)(H2O)_2]NO_32H_2O$	$AgC_{11}H_{17}N_7O_6Cl$ 548.58	1	25-90	H_2O	3.281	3.287
		2	90-249	$3H_2O$	9.47	9.86
		3	249-390	C_3H_4Cl	13.76	13.78
		4	390-760	$C_8N_3H_5$	25.88	26.11
		5	760-800	N	3.82	2.75
		Residue	>800	Ag. N_4. O_5	43.80	44.52
$[Cu(HAG)_2Cl_2].H_2O$	$CuC_{22}H_{24}N_{14}O_6Cl_3$ 784.06	1	25-62	$2H_2O$	4.25	3.202
		2	62-200	10H Cl_2	10.33	10.20
		3	200-400	5H Cl_2.	9.82	9.47
		4	400-500	5H C_7	11.35	10.90
		5	500-625	C_{12}	18.36	19.30
		6	625-700	C_3 N_5	13.51	13.13
		7	700-800	N_8 O_2	18.65	19.19
		Residue	>800	Cu O_2 N	13.97	14.59
$[Zn(HAG)\ Cl_2].H_2O$	$ZnC_{11}H_{12}N_7O_3Cl_3$ 461.14	1	25-60	$0.3H_2O$	1.40	1.30
		2	60-400	$0.7H_2O$. 5H. 1.5Cl	15.15	15.35
		3	400-475	Cl	7.69	7.72
		4	475-600	0.5Cl. 2C	9.10	9.02
		5	600-800	C_8 H_3	22.33	21.53
		Residue	>800	Zn N_7 O_2 C	44.32	45.10
$[Cd(HAG)Cl_2].2H_2O$	$CdC_{11}H_{13}N_7O_4Cl_2$ 526.47	1	25-85	H_2O	3.41	3.42
		2	85-220	H_2O .0.5 Cl	6.11	6.80
		3	220-400	$Cl_{1.5}$	10.14	10.13
		4	400-560	Cl.$C_{1.5}$. H_5	12.05	11.13
		5	560-800	$C_{9.5\ H4}$. $N_{1.5}$	27.12	26.45
		Residue	>800	Cd O_2 $N_{5.5}$	42.43	42.05

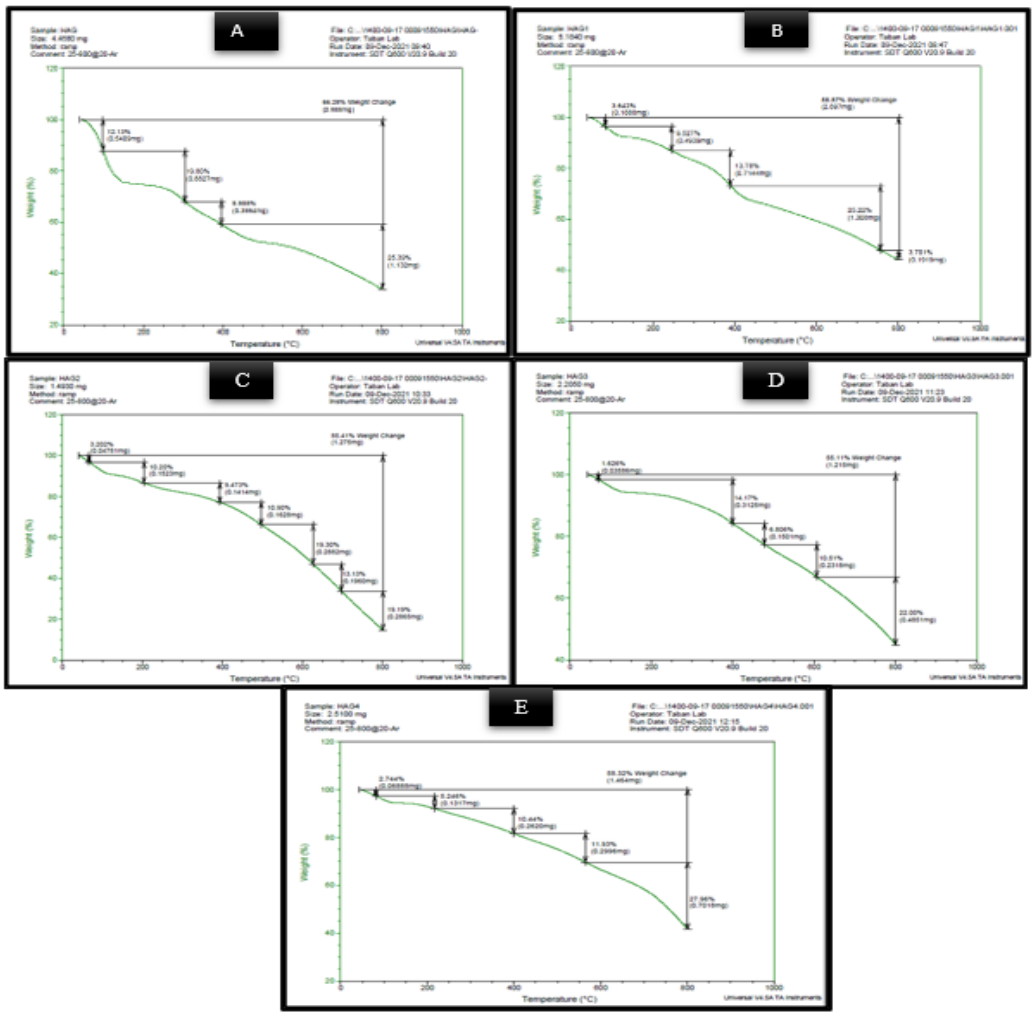

Figure 2 : Thermogram A of the HAG ligand, thermogram B for $[Ag(HAG)(H_2O)_2]$ $NO_3.2H_2O$, thermogram C for $[Cu(HAG)_2Cl_2]$, thermogram D for $[Zn(HAG)Cl_2].H_2O$, thermogram E for$[Cd(HAG)\ Cl_2].{}_2\ H_2O$ complex

3.2. FT-IR spectroscopy

FT-IR can help predict the binding mode for the HAG ligand with the metal ions in the complexes that have been generated. For identification, the FT-IR spectra of all synthesized metal ion complexes and the HAG ligand were contrasted. The spectra of the complexes showed absorption bands back to the ligands, with some variations because of the chelating. Table 5 summarizes the principal bands for the HAG ligand and its metal complexes. Figure 3 shows the highest number of moieties vibrations using the CsI disk. The following points summarize the most important information about the linkage between the metal ion and the ligands and the accompanying changes: The bands at 1573 and 1562 cm^{-1} in the HAG ligand spectrum are associated with C=N in the imidazole ring for guanine. This band's structure and position changed because of its coordination with the metal ion. The bands of O-H, N-H, and C=O [3] were unaffected in the complex spectra (Table 5). Suggesting that no chelating occurred *via* these moieties [8,9], however, small alterations in location or form were occasionally attributed to a decrease or increase in resonance because of chelating [10,11]. The azo compounds' distinct feature bands (N=N) [12]. This band appears at 1413 cm^{-1} in the spectrum of the HAG ligand. However, the stretching absorption of C-N=N-C at 1373 and 1342 cm^{-1}. The posture and intensity of these bands are minified in the complex spectra by chelating [13,14]. Several additional bands that were not present in the free-ligand spectrum were discovered. However, the most noticeable changes occurred in the 405-622 cm^{-1} range. These

bands, which appeared in this region may be related to the stretching absorptions of M-N_{azo}, M-$N_{imidazole)}$, and M-O_{H2O}. This will support our results regarding the chelation sites of the ligands with metal ions, and from the above, we conclude that the HAG ligand acts as a neutral *N*,*N*-bidentate ligand forming penta- chelating ring [15,16].

Table 5 : FT-IR spectral data (υ, cm^{-1}) bands of HAG ligand and their complexes w: weak, br: broad, s: strong, t: triple, m: medium, d: double, vw: very week.

Compound	OH	NH_2	C=O	C=N Imidazole	N=N	C-N=N-C-	M-N Imidazole	M-N azo	M-O H_2O
HAG	3472 m	3288 3170 d	1695 1672 d	1573 1562 d	1413	1373 1342 d	-	-	-
[Ag(HAG)(H_2O)$_2$]NO_3.2H_2O	3433 3328 d	3182 3110 d	1699 1654 1616 t	1544 W	1487 1458 d	1363 s	609	518 w	450 vw
[Cu(HAG)$_2$ Cl_2].H_2O	3435 3353 d-br	3193 3112 d	1695 1674 d	1612 1564 D	1415 1377 d	1315 w	605	514 w	462 vw
[Zn(HAG) Cl_2].H_2O	3447 b	3220 3197 d	1699 1670 d	1610 1568 D	1460 1419 1375	1340 w	601 w	503 W	325
[Cd(HAG) Cl_2].2 H_2O	3340 w	3178 3118 d-w	1697 1674 d	1560 M	1475 1458 1417 t	1375 w	622 605 d-w	500 vw	415.5 vw

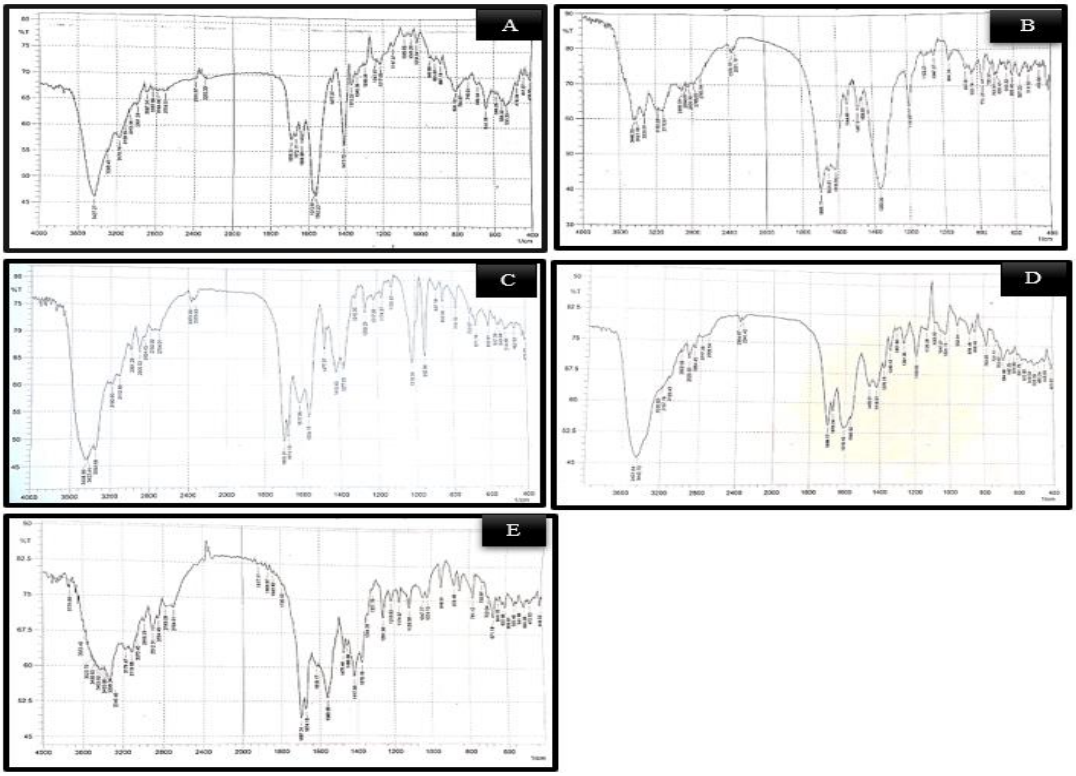

Figure 3: FT-IRspectra of the (A) HAG ligand (B) [Ag (HAG) $(H_2O)_2$]NO_3.$2H_2O$ (C) [$Cu(HAG)_2Cl_2$] (D) [Zn(HAG) Cl_2].H2O (E) [Cd(HAG) Cl_2].$2H_2O$ complexes

3.3. ^{1}H NMR spectroscopy

The ^{1}H NMR spectral data of the HAG ligand in DMSO-d6 solvent (Figures 4) [17,18] are listed in Table 6 [19]. The signal at 2.50 ppm belongs to the deuterated DMSO solvent [20]

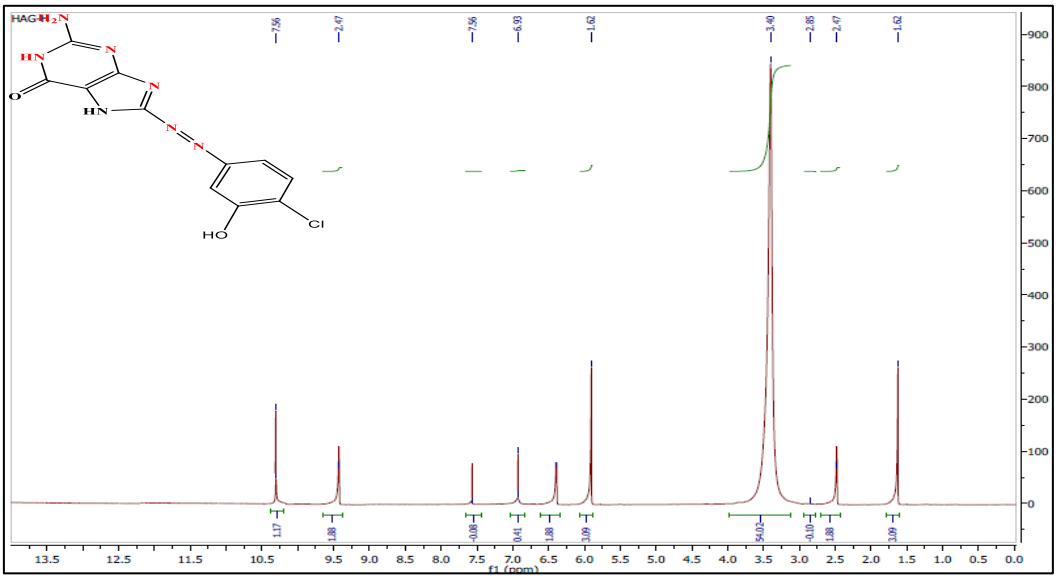

Figure 4: ^{1}H NMR spectrum of the HAG ligand

Table 6 : ^{1}H NMR spectral data (□, ppm) of the HAG ligand

Compound	1H, NH imidazole	1H, OH	4H, Ar-H	2H, NH_2
HAG	10.25	9.50	6.62-7.02	6.63

3.4. The electronic spectrum of the HAG ligand and its complexes and the magnetic properties

The electronic spectrum of the HAG ligand in water [10^{-4} M] with a range of 280-1100 nm is given in Figure 5. There are two bands: the first band ($\pi \rightarrow \pi*$) at (293 nm, 34129 cm^{-1}) has been linked to the intramolecular transition of heterocyclic and aromatic moieties [21]. The second band was observed at 339 nm - 29498 cm^{-1} ($\pi \rightarrow \pi^*$), which was attributed to an intramolecular charge transfer that occurred *via* the carbonyl and azo moieties. Sharp absorption bands in the electronic spectra of the diamagnetic (d^{10}) Ag(I), Cd(II), and Zn(II) complexes (Figures 5B, D, and E) were identified as the charge transfer CT [22,23]. The electronic spectra of the $[Cu(HAG)_2Cl_2]$ H_2O complex (Figure 5C) are $\upsilon^1 = [^2B_1g \rightarrow {}^2A_1g]$ (904 nm, 11061 cm^{-1}) and $\upsilon^2 = [^2B_1g \rightarrow {}^2B_2g]$ (798 nm, 12531 cm^{-1}). The charge transfer occurred at 597 - 16750 cm^{-1}, while $\upsilon^3 = [^2B_1g \rightarrow {}^2Eg]$ was concealed beneath this band. This is a defining feature of a distorted octahedral because of the Jahn-Teller distortion (D_{4h}). The magnetic moment is 1.33 B.M.

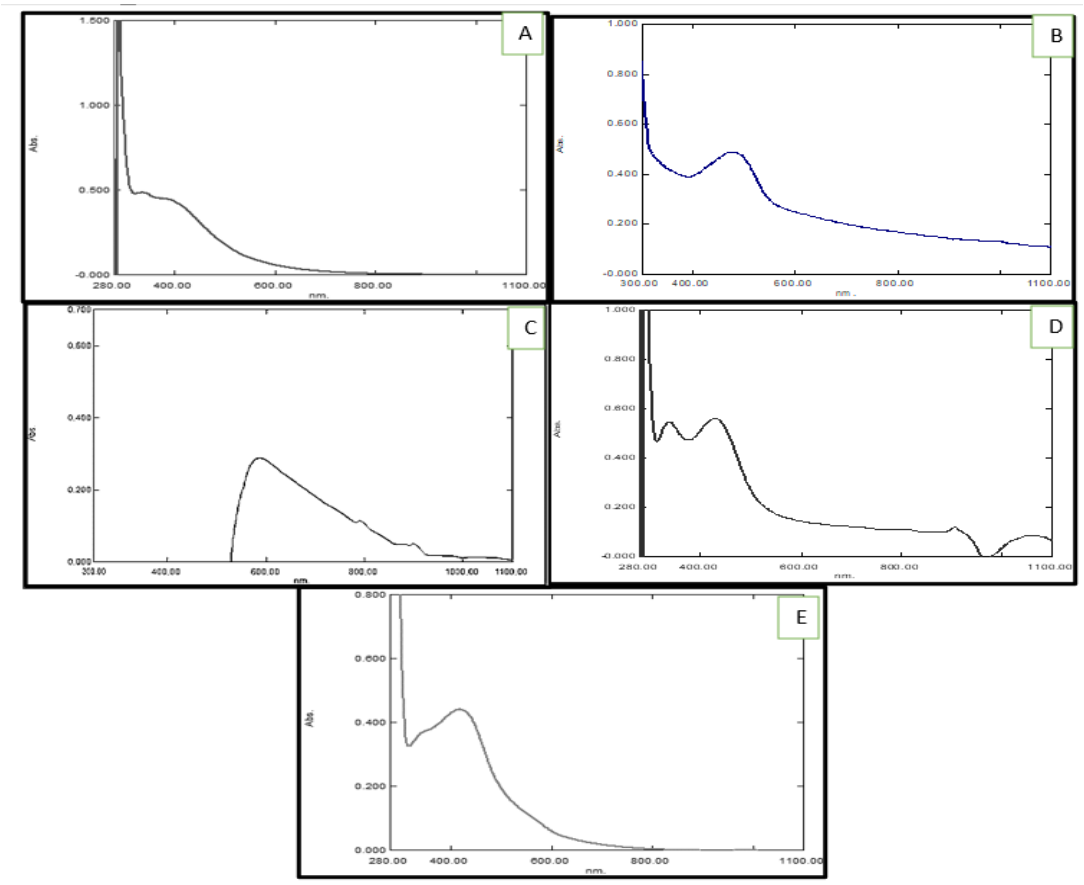

Figure 5 : The electronic spectra for HAG ligand (A), $[Ag(HAG)(H_2O)_2]NO_3.2H_2O$ complex (B), $[Cu(HAG)_2Cl_2]$ complex (C), $[Zn(HAG)\ Cl_2].H_2O$ complex (D), $[Cd(HAG)\ Cl_2].2H_2O$ complex (E)

Table 7: The data of the spectrum of UV-Vis for HAG ligand and their complexes

Compound	λ(*nm*)	Wavenumber (cm^{-1})	Assignment	hybridization	Geometry
HAG	293 339	34129 29498	$\pi \rightarrow \pi *$ $\pi \rightarrow \pi^*$	-	-
$[Ag(HAG)(H_2O)_2]NO_3.2H_2O$	467	22371	CT	sp^3	Tetrahedral
$[Cu(HAG)_2Cl_2].H_2O$	904 798 597	11061 12531 16750	$2B_1g \rightarrow 2A_1g$ $B_1g \rightarrow 2B_2g_2$ CT	sp^3d^2	Distorted octahedral
$[Zn(HAG)Cl_2].H_2O$	334	29994	CT	sp^3	Tetrahedral
$[Cd(HAG)Cl_2].2H_2O$	418	23923	CT	sp^3	Tetrahedral

3.5. Dying performance

The effectiveness of the HAG ligands' complex dyes on wool was examined. Most protein filaments that make up wool fibers have complex structure amino groups and are called keratin. It has the general formula [$H_2N.CHR.COOH$], where R is an independent chain with a distinct character, and is composed of lengthy polypeptide chains with 18 different amino acids. The bridges are composed of cysteine and connect chains [24]. These theories provided a holistic explanation strictly in terms of the ionic theory [25], the mechanism of wool dyeing under acidic conditions, interactions with the fibers' positively charged amino groups, and the colored anions with a negative charge [26]. The placement of the substituted present, the diazotized chemical, and the outcomes cause differences in the tones of the azo dye textile. Grayscale tests were performed on the complexes chosen for color fastness and standing time. The replicas were colored with a fixative, the color fastness of the fabrics was evaluated during washing using soap powder (2%) at 260 °C for 30 minutes, and the responsiveness was excellent to water (Table 9). The HAG ligand and its complexes have various colors when used for dying wool fiber (Figure 8).

Figure 8 : The dying of HAG ligand and some of their complexes (HAG = Ligand, HAG1 = $[Ag(HAG)(H2O)_2]NO_3.2H_2O$, HAG2 = $[Cu(HAG)_2Cl_2].H_2O$, HAG3 = $[Zn(HAG)Cl_2].H_2O$, HAG4 = $[Cd(HAG)Cl_2].2H_2O$

Table 9 : Dying properties

Compounds	Color	Color fastness	Staining dye	Notes
HAG	Brown	4	4	Acceptable on grayscale
$[Cu(HAG)_2Cl_2].H_2O$	Green	3	3	Acceptable on grayscale

Where the values 4-5 are good, 3 is moderate, and 1-2 are not good. According to woolen textile standard No. 3616

Table 10 : The data of acid-base titrations of HAG ligand

No.	Volume of acid (mL)	Volume of NaOH (mL)	Volume of $NaHCO_3$) (mL)	Color in acid	Color in base
1	5.0 (HCl)	6.5	-	Yellow	Colorless
2	5.0 (ACOH)	7	-	Yellow	Colorless
	Titration of acid (0.1M) against NaHCO3 (0.1M) for (HAG)				
3	5.0 (HCl)	-	5.5	Yellow	Light-yellow
4	5.0 (ACOH)	-	5.0	Light-yellow	Light-yellow

3.6. Azo dyes as acid-base indicators

The organic dyes with distinct colors in solutions with different pH values are known as acid-base indicators. They are frequently used in acid-base titrations to establish the equivalency point. When the pH changes, they exhibited a striking color change. Due to their capacity to alter color in response to pH, azo dyes are the most widely used chemical molecules as acid-base indicators [27,28]. As a result, acid-base titrations were used to test this feature in all azo dyes . All synthetic azo dyes exhibited reversible and abrupt color changes when transitioning from an acidic condition to a basic condition or vice versa. They also possessed a stable color in both acidic and basic solutions. Each azo compound accurately identified the endpoint. Table 10 shows the data of acid-base titrations that are used to assess the indicator property of azo dyes that should be included. Figure 9 displays the hues of azo dye solutions in both acidic and basic environments.

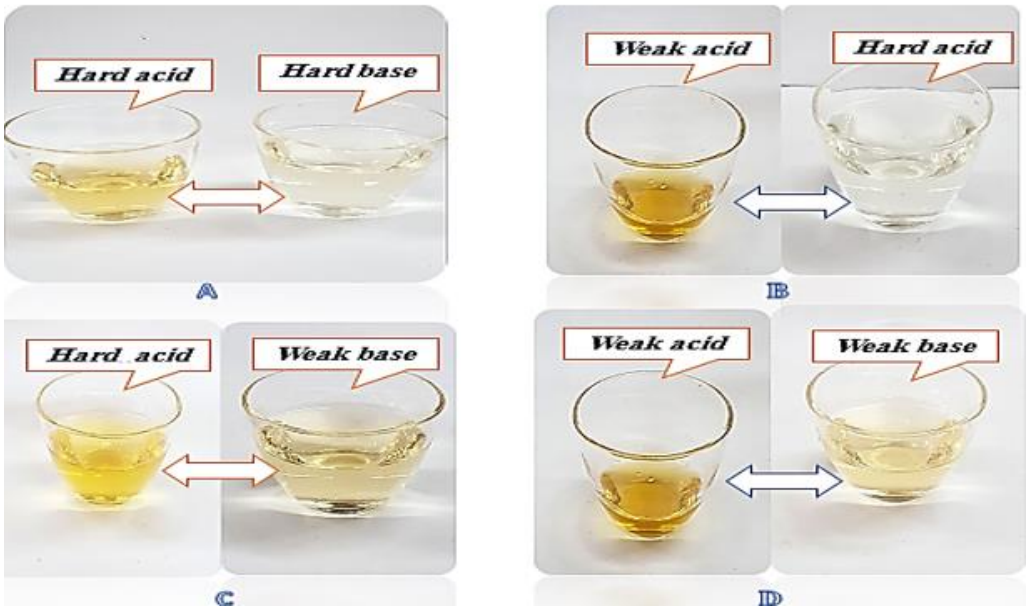

Figure 9: The change in the color of azo ligand (HAG): A = HCl with NaOH B = ACOH with NaOH, C = HCl with $NaHCO_3$, D = ACOH with $NaHCO_3$

3.6. Photostability

By dissolving the HAG ligand in water at a concentration of (10^{-4}M) and subjecting them to ultraviolet (UV) radiation for two hours at room temperature, their photostability was examined (Table 11). The photostability was calculated [15,29] using the difference between the initial absorbance (i.e., before irradiation and the final absorbance to the beginning absorbance). The following findings were obtained from the photostability test:

HAG > $[Cu(HAG)_2\ Cl_2].H_2O$ > $[Cd(HAG)Cl_2].2H_2O$ > $[Zn(HAG)Cl_2].H_2O$ > $[Ag(HAG)(H_2O)_2]NO_3.2H_2O$

Table 11: The photostability data of HAG ligand and its complexes

Compounds	Time (minutes)	Absorbance (nm)	Photostability Percentage (%)
HAG	0	2.111	5.49
	10	2.109	
	20	2.108	
	30	2.107	
	40	2.105	
	60	2.105	
	75	2.103	
	90	2.100	
	105	2.100	
	120	1.995	
$[Ag(HAG)(H_2O)_2]NO_3.2H_2O$	0	0.385	1.03
	10	0.379	
	20	0.378	
	30	0.377	
	40	0.378	
	60	0.378	
	75	0.378	
	90	0.380	
	105	0.380	
	120	0.381	
$[Cu(HAG)_2 Cl_2].H_2O$	0	1.950	1.19
	10	1.945	
	20	1.944	
	30	1.942	
	40	1.943	
	60	1.944	
	75	1.940	
	90	1.939	
	105	1.933	
	120	1.927	
$[Zn(HAG)Cl_2].H_2O$	0	2.017	1.09
	10	2.017	
	20	2.017	
	30	2.010	
	40	2.009	
	60	2.011	
	75	2.011	
	90	1.998	
	105	1.996	
	120	1.995	
$[Cd(HAG)Cl_2].2H_2O$	0	1.750	1.14
	10	1.741	

	20	1.737
	30	1.740
	40	1.740
	60	1.740
	75	1.739
	90	1.739
	105	1.735
	120	1.730

4. Conclusion

Different spectroscopic techniques are used to characterize and study Ag(I), Cu(II), Zn(II), and Cd(II) complexes that are formed from the HAG azo ligand (2-amino-8-((4-chloro-3-hydroxyphenyl)diazenyl)-1,7-dihydro-6H-purin-6-one). The complexes formed at different stoichiometric rates. All have tetrahedral geometry with the exception of the Cu(II) complex, which has a distorted octahedral structure, and the ligand acts as a bidentate ligand. It can also be used as an indicator for the titrimetric assay in both strong acid/strong base and weak acid/strong base titrimetric analyses. The ligand and its complexes have various colors confirmed to be used to dye wool fabrics. The ultraviolet protection factor's findings support the material's excellent UV absorption capacity to support various analytical works in teaching and research laboratories, which remains our goal.

References

[1] K. Barman and S. J. R. A. Jasimuddin, "Electrochemical detection of adenine and guanine using a self-assembled copper (II)-thiophenyl-azo-imidazole complex monolayer modified gold electrode," *RSC Advances*, vol. 4, no. 91, pp. 49819-49826, 2014.

[2] C. A. Shukla, M. S. Kute, and A. Kulkarni, "Towards sustainable continuous production of azo dyes: possibilities and techno-economic analysis," *Green Chemistry*, vol. 23, no. 17, pp. 6614-6624, 2021.

[3] S. Prakash, G. Somiya, N. Elavarasan, K. Subashini, S. Kanaga, R. Dhandapani, M. Sivanandam, P. Kumaradhas, C. Thirunavukkarasu, and V. Sujath, "Synthesis and characterization of novel bioactive azo compounds fused with benzothiazole and their versatile biological applications," *Journal of Molecular Structure*, vol. 1224, pp. 129016-129042, 2021.

[4] A. K. Sarangi and B Mohapatra, "Synthesis and characterization of some binuclear metal complexes with a pentadentate azodye ligand: an experimental and theoretical study," *Applied Organometallic Chemistry*, vol. 34, no. 8, p. e5693-20, 2020.

[5] S. Ghattavi and A. Nezamzadeh-Ejhieh, "A visible light driven AgBr/g-C3N4 photocatalyst composite in methyl orange photodegradation: focus on photoluminescence, mole ratio, synthesis method of g-C3N4 and scavengers," *Composites Part B: Engineering*, vol. 183, p. 107712-107716, 2020.

[6] J. O. Park., "Metabolite concentrations, fluxes and free energies imply efficient enzyme usage," *Nature chemical biology*, vol. 12, no. 7, pp. 482-489, 2016.

[7] M. Gaber, N. El-Wakiel, and O. M. Hemeda, "Cr(III), Mn(II), Co(II), Ni(II) and Cu(II) complexes of 7-((1H-benzo[d]imidazol-2-yl)diazenyl)-5-nitroquinolin-8-ol. synthesis, thermal, spectral, electrical measurements, molecular modeling and biological activity," *Journal of Molecular Structure*. vol. 1180, pp. 318-329, 2019.

[8] M. S. Masoud, A. E. Ali, G. S. Elasala, and S. H. Kolkaila, "Spectroscopic studies and thermal analysis on cefoperazone metal complexes," *J. Chem. Pharm. Res*, vol. 9, no. 4, pp. 171-179, 2017.

[9] K. J. Al-Adilee and H. M. H. Al-Muaeni, "Synthesis, identification, structural, studies and biological activity of some transition metal complexes with novel heterocyclic azo-Schiff base ligand derived from benzimidazole," *J. Chem. Pharm. Res*, vol. 7, no. 8, pp. 89-103, 2015.

[10] N. Mallikarjuna, J. Keshavayya, M. Maliyappa, R. S. Ali, and Venkatesh, "Synthesis, characterization, thermal and biological evaluation of Cu(II), Co(II) and Ni(II) complexes of azo dye ligand containing sulfamethaxazole moiety," *Journal of Molecular Structure*, vol. 1165, pp. 28-36, 2018.

[11] S. R. Rasool, N. M. Aljamali, and A. J. Al-Zuhairi, "Guanine substituted heterocyclic derivatives as bioactive compounds," *Biochem. Cell. Arch*, vol. 20, no. Supplement 2, pp. 3651-3655, 2020.

[12] R. A. Dabish and A. Khider, "Synthesis and spectral studies of some new complexes containing azo ligand with anticancer, antibacterial and dyeing performance," *Annals of the Romanian Society for Cell Biology*, vol. 25, no. 4, pp. 7968-8006, 2021.

[13] M. Bouhdada and M. Amane, "Synthesis, characterization and spectroscopic properties of the hydrazodye and new hydrazodye-metal complexes," *Journal of Molecular Structure*, vol. 1150, pp. 419-426, 2017

[14] K. D. Patel and Hasmukh S. Patel, "Synthesis, spectroscopic characterization and thermal studies of some divalent transition metal complexes of 8-hydroxyquinoline," *Arabian Journal of Chemistry*, vol. 10, pp. S1328-S1335, 2017.

[15] J. R. Štoček and M. J. B. Dračínský, "Tautomerism of guanine analogues," *Biomolecules* vol. 10, no. 2, p. 170, 2020.

[16] H. A. Bayoumi, A. Alaghaz, and M. S. Aljahdali, "Cu(II), Ni(II), Co(II) and Cr(III) complexes with N_2O_2-chelating schiff's base ligand incorporating azo and sulfonamide moieties: spectroscopic, electrochemical behavior and thermal decomposition studies," *International Journal of Electrochemical Science*, vol. 8, pp. 9399-9413, 2013.

[17] A. Jantschke, I. Pinkas, A. Hirsch, N. Elad, A. Schertel, L. Addadi, and S.Weiner, "Anhydrous β-guanine crystals in a marine dinoflagellate: Structure and suggested function," *Journal of Structural Biology*, vol. 207, no. 1, pp. 12-20, 2019.

[18] W. A. Mahmoud, A. A. M. Ali, and T. A. Kareem, "Preparation and spectral characterization of new azo imidazole ligand 2-[(2-cyano phenyl) Azo]-4, 5-diphenyl imidazole and its complexes with Co(II), Ni(II), Cu(II), Zn(II), Cd(II) and Hg(II) ions," *Baghdad Science Journal*, vol. 12, no. 1, pp. 96-109, 2015.

[19] A. Bamoniri, A. Pourali, and S. M. R. Nazifi, "Nano Silica/HIO_4 as a green and reusable catalyst for synthesis of 2-naphthol azo dyes under grinding conditions," International *Journal of Nanoscience and Nanotechnology*, vol. 10, no. 4, pp. 197-203, 2014.

[20] D. M. Lewis and J. A. Rippon, *The coloration of wool and other keratin fibres*. John Wiley and Sons, 2013.

[21] J. Cai, H. Jiang, W. Chen, and Z. Cui, "Design, synthesis, characterization of water-soluble indophenine dyes and their application for dyeing of wool, silk and nylon fabrics," *Dyes and Pigments*, vol. 179, p. 108385, 2020.

[22] S. M. Al-Majidi and M. G. Al-Khuzaie, "Synthesis and characterization of new azo compounds linked to 1,8-naphthalimide and studying their ability as acid-base indicators," *Iraqi Journal of Science*, vol. 60, no.11, pp. 2341-2352, 2019.

[23] A. Abbas, "Preparation, characterization and biological evaluation of some lanthanide (III) ions complexes with 3-(1-methyl-2-benzimidazolylazo)-tyrosine," *Baghdad Science Journal*, vol. 13, no. 2, pp. 1-17, 2016.

[24] A. Abbas, "Lanthanide ions complexes of 2-(4-amino antipyrine)-L-tryptophane (AAT): Preparation, Identification and Antimicrobial Assay," *Iraqi Journal of Science*, vol. 56, no. 4C, pp. 3297-309, 2015.

[25] Z. A. Sallal and H. T. Ghanem, "Synthesis and identification of new oxazepine derivatives bearing azo group in their structures," *Iraqi Journal of* Science, vol. 59, no.1A, pp. 1-8, 2018.

[26] S. M. Kadhim and S. M. Mahdi, "Preparation and characterization of new (lalogenated azo-Schiff) ligands with some of their transition metal ions complexes," *Iraqi Journal of Science*, vol. 63, no. 8, pp. 3283-3299, 2022.

[27] K. S. Khashan, G. M. Sulaiman, and S. A Hussain, "Synthesis and characterization of aluminum doped zinc oxide nanostructures by Nd: YAG laser in liquid," *Iraqi Journal of Science*, vol. 61, no. 10, pp. 2590-2598, 2020.

[28] A. M. Al-Azzawi and E. K. Jassem, "Synthesis and characterization of several new succinimides linked to phenyl azo benzothiazole or thiazole moieties with expected biological activity," *Iraqi Journal of Science*, vol. 57, no. 1C, pp. 534-544, 2016.

[29] B. U. Erika. S. Batagin-Neto and A. X. Graeff, "Synthesis and characterization of melanin in DMSO. "*Journal of Molecular Structure*, vol. 1047, pp. 102-108, 2013.